Discontinuous Galerkin discretizations of optimized Schwarz methods for solving the time-harmonic Maxwell equations

Mohamed El Bouajaji, Victorita Dolean, Martin J. Gander, Stéphane Lanteri, Ronan Perrussel

DISCONTINUOUS GALERKIN DISCRETIZATIONS OF OPTIMIZED SCHWARZ METHODS FOR SOLVING THE TIME-HARMONIC MAXWELL EQUATIONS

M. EL BOUAJAJI* V. DOLEAN† M.J. GANDER‡ AND S. LANTERI* R. PERRUSSEL‡

Abstract. We show in this paper how to properly discretize optimized Schwarz methods for the time-harmonic Maxwell equations using a discontinuous Galerkin (DG) method. Due to the multiple traces between elements in the DG formulation, it is not clear a priori how the more sophisticated transmission conditions in optimized Schwarz methods should be discretized, and the most natural approach does not lead at convergence of the Schwarz method to the mono-domain DG discretization, which implies that for such discretizations, the DG error estimates do not hold when the Schwarz method has converged. We present an alternative discretization of the transmission conditions in the framework of a DG weak formulation, and prove that for this discretization the multidomain and mono-domain solutions for the Maxwell's equations are the same. We illustrate our results with several numerical experiments of propagation problems in homogeneous and heterogeneous media.

Key words. computational electromagnetism, time-harmonic Maxwell's equations, Discontinuous Galerkin method, optimized Schwarz methods, transmission conditions.

AMS subject classifications. 65M55, 65F10, 65N22

1. Introduction. Discontinuous Galerkin (DG) methods have received a lot of attention over the last decade, since they combine the best of both finite element and finite volume methods. The approximation of each field is done locally at the level of each mesh element, by using a local basis of functions, and the discontinuity between neighboring elements is treated using a finite volume flux. A richer representation of the solution is given, at the price of increasing the total number of degrees of freedom as a result of the decoupling of the elements. The literature on these methods applied to different types of equations is rich and we will focus on contributions concerning Maxwell's equations. A complete historical introduction with a large panel of references can be found in the milestone book on DG methods by Hesthaven and Warburton [24].

Theoretical results on DG methods applied to the time-harmonic Maxwell equations have been obtained by several authors. Most of these use the second order formulation of the Maxwell equations. An alternative is to use the first order formulation as in [21, 22, 23], based on the theory of the Friedrichs systems. In a large part of the literature on time-harmonic problems, a mixed formulation is used (see [31, 26]), but DG methods on the non-mixed formulation like interior penalty techniques [25, 6] and local discontinuous Galerkin methods [6] have also been studied. A numerical convergence study of discontinuous Galerkin methods based on centered and upwind fluxes and nodal polynomial interpolation applied to the first-order time-harmonic Maxwell system in the two-dimensional case can be found in [12].

*INRIA SOPHIA ANTIPOLIS-MÉDITERRANÉE, 06902 SOPHIA ANTIPOLIS CEDEX, FRANCE.

†UNIV. DE NICE SOPHIA-ANTIPOLIS, LABORATOIRE J.-A. DIEUDONNÉ, NICE, FRANCE. DOLEAN@UNICE.FR

‡SECTION DE MATHÉMATIQUES, UNIVERSITÉ DE GENÈVE, CP 64, 1211 GENÈVE, MARTIN.GANDER@MATH.UNIGE.CH

*INRIA SOPHIA ANTIPOLIS-MÉDITERRANÉE, 06902 SOPHIA ANTIPOLIS CEDEX, FRANCE.

‡CNRS, UNIVERSITÉ DE TOULOUSE, LABORATOIRE PLASMA ET CONVERSION D'ÉNERGIE, 31071 TOULOUSE CEDEX 7, FRANCE

Like for all other discretizations of the time-harmonic Maxwell equations, it is also difficult to solve linear systems obtained by DG discretizations with iterative methods. Due to the indefinite nature of the problems, classical iterative solvers fail as in the Helmholtz case [19]. Després defined in [9] a first provably convergent domain decomposition algorithm for the Helmholtz equation. This algorithm was extended to Maxwell's equations in [10]. Even better transmission conditions were proposed in [7, 8, 20], based on optimized Schwarz theory, with an application to the second order Maxwell system in [1]. An entire hierarchy of optimized Schwarz methods for the first order Maxwell's equations can be found in [15], with complete asymptotic results for the optimization. First DG discretizations of optimized Schwarz methods for time-harmonic Maxwell's equations were proposed in [17] and [4]. Classical finite-element based non-overlapping and non-conforming domain decomposition methods for the computation of multiscale electromagnetic radiation and scattering problems can be found in [27, 30, 28, 32, 33, 29].

This paper is organized as follows: in Section 2 we present the time-harmonic Maxwell equations as a first order system, and introduce the notation for what follows. In Section 3 we show the classical and optimized Schwarz algorithm at the continuous level for the first order Maxwell system. In Section 4, we introduce a weak formulation for the first order system, and then use a DG approximation to obtain discrete subdomain problems. We then show that while the DG discretization of the classical Schwarz method is very natural, optimized transmission conditions are more tricky to discretize, and we present a discretization for which we prove that the monodomain and multidomain formulations are equivalent. We then show in Section 5 several numerical experiments for both homogeneous and heterogeneous propagation problems to illustrate the performance of the optimized Schwarz methods as solvers for DG discretized Maxwell equations. Section 6 contains a brief conclusion.

2. The Time Harmonic Maxwell System. The time-harmonic Maxwell equations in a homogeneous medium are given by

$$i\omega\varepsilon\mathbf{E} - \operatorname{curl}\mathbf{H} + \sigma\mathbf{E} = \mathbf{0}, \qquad i\omega\mu\mathbf{H} + \operatorname{curl}\mathbf{E} = \mathbf{0}, \tag{2.1}$$

where the positive real parameter ω is the pulsation of the harmonic wave, σ is the electric conductivity, ε is the electric permittivity, μ magnetic permeability and the unknown complex-valued vector fields $\mathbf{E}$ and $\mathbf{H}$ are the electric and magnetic fields. In the homogeneous case to simplify the notation we can rewrite equation 2.1 as

$$i\tilde{\omega}\mathbf{E} - \operatorname{curl}\mathbf{H} + \tilde{\sigma}\mathbf{E} = 0, \qquad i\tilde{\omega}\mathbf{H} + \operatorname{curl}\mathbf{E} = \mathbf{0}, \tag{2.2}$$

where $\tilde{\omega} := \omega\sqrt{\varepsilon\mu}$ and $\tilde{\sigma} := \sigma\sqrt{\frac{\mu}{\varepsilon}}$. Collecting the variables into one big vector $\mathbf{W} := (\mathbf{E}, \mathbf{H})$, we can rewrite (2.2) as a first order system,

$$G_0\mathbf{W} + G_x\partial_x\mathbf{W} + G_y\partial_y\mathbf{W} + G_z\partial_z\mathbf{W} = 0, \tag{2.3}$$

where

$$G_0 := \begin{pmatrix} (\tilde{\sigma} + i\tilde{\omega})\mathbb{I}_{3\times3} & 0_{3\times3} \\ 0_{3\times3} & i\tilde{\omega}\mathbb{I}_{3\times3} \end{pmatrix},$$

and

$$G_x := \begin{pmatrix} 0_{3\times3} & N_x \\ N_x^T & 0_{3\times3} \end{pmatrix}, \quad G_y := \begin{pmatrix} 0_{3\times3} & N_y \\ N_y^T & 0_{3\times3} \end{pmatrix}, \quad G_z := \begin{pmatrix} 0_{3\times3} & N_z \\ N_z^T & 0_{3\times3} \end{pmatrix},$$

with

$$N_x := \begin{pmatrix} 0 & 0 & 0 \\ 0 & 0 & 1 \\ 0 & -1 & 0 \end{pmatrix}, \quad N_y := \begin{pmatrix} 0 & 0 & -1 \\ 0 & 0 & 0 \\ 1 & 0 & 0 \end{pmatrix}, \quad N_z := \begin{pmatrix} 0 & 1 & 0 \\ -1 & 0 & 0 \\ 0 & 0 & 0 \end{pmatrix}.$$

For a general vector $\mathbf{n} = (n_x, n_y, n_z)$, we can define the matrices

$$G_{\mathbf{n}} := \begin{pmatrix} 0_{3\times 3} & N_{\mathbf{n}} \\ N_{\mathbf{n}}^T & 0_{3\times 3}, \end{pmatrix} \quad \text{and} \quad N_{\mathbf{n}} := \begin{pmatrix} 0 & n_z & -n_y \\ -n_z & 0 & n_x \\ n_y & -n_x & 0 \end{pmatrix}.$$

The skew-symmetric matrix $N_{\mathbf{n}}$ allows us to define the cross product between a vector $\mathbf{V}$ and the vector $\mathbf{n}$,

$$\mathbf{V} \times \mathbf{n} = N_{\mathbf{n}}\mathbf{V} \text{ and } \mathbf{n} \times \mathbf{V} = N_{\mathbf{n}}^T\mathbf{V}. \tag{2.4}$$

Moreover, if the vector $\mathbf{n}$ is normalized, we have also $N_{\mathbf{n}}^3 = -N_{\mathbf{n}}$. Using these notations, the matrices G_l with l standing for $\{x, y, z\}$ are in fact $G_l = G_{\mathbf{e}_l}$, where $\mathbf{e}_l$, $l = 1, 2, 3$ are the canonical basis vectors.

We consider here a *total field* formulation, that is we are interested in the unknown vector $\mathbf{W} = \mathbf{W}_{\text{inc}} + \mathbf{W}_{\text{sc}}$ where $\mathbf{W}_{\text{inc}}$ represents the *incident field* and $\mathbf{W}_{\text{sc}}$ represents the *scattered field* over an obstacle with boundary Γ_m or in an inhomogeneous medium. Our goal is to solve the boundary-value problem whose strong form is given by

$$\begin{array}{rcll} G_0\mathbf{W} + \displaystyle\sum_{l\in\{x,y,z\}} G_l\partial_l\mathbf{W} & = & 0, & \text{in } \Omega, \\ (M_{\Gamma_m} - G_{\mathbf{n}})\mathbf{W} & = & 0 & \text{on } \Gamma_m, \\ (M_{\Gamma_a} - G_{\mathbf{n}})(\mathbf{W} - \mathbf{W}_{\text{inc}}) & = & 0 & \text{on } \Gamma_a. \end{array} \tag{2.5}$$

Here the matrices M_{Γ_m} and M_{Γ_a} are used for taking into account the boundary conditions of the problem imposed on the *metallic* boundary Γ_m and the *absorbing* boundary Γ_a,

$$M_{\Gamma_m} = \begin{pmatrix} 0_{3\times 3} & N_{\mathbf{n}} \\ -N_{\mathbf{n}}^T & 0_{3\times 3} \end{pmatrix} \text{ and } M_{\Gamma_a} = |G_{\mathbf{n}}| = \begin{pmatrix} N_{\mathbf{n}}N_{\mathbf{n}}^T & 0_{3\times 3} \\ 0_{3\times 3} & N_{\mathbf{n}}^T N_{\mathbf{n}} \end{pmatrix}.$$

We will use in what follows the matrices $G_{\mathbf{n}}^+$ and $G_{\mathbf{n}}^-$ which denote the positive and negative parts of $G_{\mathbf{n}}$ according to its diagonalization. We note that $|G_{\mathbf{n}}| = G_{\mathbf{n}}^+ - G_{\mathbf{n}}^-$ and the definition of the $G_{\mathbf{n}}^+$ and $G_{\mathbf{n}}^-$ can be deduced from those of $G_{\mathbf{n}}$ and $|G_{\mathbf{n}}|$,

$$G_{\mathbf{n}}^- = \frac{1}{2}(G_{\mathbf{n}} - |G_{\mathbf{n}}|) \text{ and } G_{\mathbf{n}}^+ = \frac{1}{2}(G_{\mathbf{n}} + |G_{\mathbf{n}}|). \tag{2.6}$$

3. Continuous classical and optimized Schwarz algorithms. We decompose the computational domain Ω into two non-overlapping subdomains Ω_1 and Ω_2. We denote by Σ the interface between Ω_1 and Ω_2, by $\mathbf{W}_j$ the restriction of $\mathbf{W}$ to the subdomain Ω_j and by $\mathbf{n}$ the unit outward normal vector to Σ pointing from Ω_1 to Ω_2. Schwarz algorithms compute at each iteration step $n = 0, 1, 2, ...$ a new approximation $\mathbf{W}_j^{n+1}$ from a given approximation $\mathbf{W}_j^n$, $j = 1, 2$ by solving

$$\begin{array}{rcll} G_0\mathbf{W}_1^{n+1} + \displaystyle\sum_{l\in\{x,y,z\}} G_l\partial_l\mathbf{W}_1^{n+1} & = & 0, & \text{in } \Omega_1, \\ (G_{\mathbf{n}}^- + S_1G_{\mathbf{n}}^+)\mathbf{W}_1^{n+1} & = & (G_{\mathbf{n}}^- + S_1G_{\mathbf{n}}^+)\mathbf{W}_2^n, & \text{on } \Sigma, \\ G_0\mathbf{W}_2^{n+1} + \displaystyle\sum_{l\in\{x,y,z\}} G_l\partial_l\mathbf{W}_2^{n+1} & = & 0, & \text{in } \Omega_2, \\ (G_{\mathbf{n}}^+ + S_2G_{\mathbf{n}}^-)\mathbf{W}_2^{n+1} & = & (G_{\mathbf{n}}^+ + S_2G_{\mathbf{n}}^-)\mathbf{W}_1^n, & \text{on } \Sigma, \end{array} \tag{3.1}$$

where S_1 and S_2 are differential operators. When S_1 and S_2 are equal to zero, the algorithm is called *classical Schwarz algorithm* and it uses *classical transmission conditions*. It has been shown in [15] that these classical conditions have the meaning of imposing Dirichlet conditions on characteristic (incoming) variables in each subdomain. Since

$$G_{\mathbf{n}}^{-} = \begin{pmatrix} -N_{\mathbf{n}}N_{\mathbf{n}}^T & N_{\mathbf{n}} \\ N_{\mathbf{n}}^T & -N_{\mathbf{n}}^T N_{\mathbf{n}} \end{pmatrix} = \begin{pmatrix} \mathbb{I}_{3\times 3} \\ -N_{\mathbf{n}}^T \end{pmatrix} \begin{pmatrix} -N_{\mathbf{n}}N_{\mathbf{n}}^T & N_{\mathbf{n}} \end{pmatrix}, \tag{3.2}$$

$$G_{\mathbf{n}}^{+} = \begin{pmatrix} N_{\mathbf{n}}N_{\mathbf{n}}^T & N_{\mathbf{n}} \\ N_{\mathbf{n}}^T & N_{\mathbf{n}}^T N_{\mathbf{n}} \end{pmatrix} = \begin{pmatrix} \mathbb{I}_{3\times 3} \\ N_{\mathbf{n}}^T \end{pmatrix} \begin{pmatrix} N_{\mathbf{n}}N_{\mathbf{n}}^T & N_{\mathbf{n}} \end{pmatrix}, \tag{3.3}$$

the classical transmission conditions are also equivalent to imposing impedance conditions,

$$\begin{aligned} G_{\mathbf{n}}^{-}\mathbf{W}_1^{n+1} = G_{\mathbf{n}}^{-}\mathbf{W}_2^{n} \quad &\Longleftrightarrow \quad \mathcal{B}_{\mathbf{n}}(\mathbf{E}_1^{n+1}, \mathbf{H}_1^{n+1}) = \mathcal{B}_{\mathbf{n}}(\mathbf{E}_2^{n}, \mathbf{H}_2^{n}), \\ G_{\mathbf{n}}^{+}\mathbf{W}_2^{n+1} = G_{\mathbf{n}}^{+}\mathbf{W}_1^{n} \quad &\Longleftrightarrow \quad \mathcal{B}_{-\mathbf{n}}(\mathbf{E}_2^{n+1}, \mathbf{H}_2^{n+1}) = \mathcal{B}_{-\mathbf{n}}(\mathbf{E}_1^{n}, \mathbf{H}_1^{n}), \end{aligned} \tag{3.4}$$

where the impedance operator is given by

$$\mathcal{B}_{\mathbf{n}}(\mathbf{E}, \mathbf{H}) := N_{\mathbf{n}}N_{\mathbf{n}}^T\mathbf{E} - N_{\mathbf{n}}\mathbf{H}, \tag{3.5}$$

and for subdomain Ω_2 we have used the fact that $G_{\mathbf{n}}^{+} = -G_{-\mathbf{n}}^{-}$. The classical Schwarz algorithm has been thoroughly tested in [16] for the solution of the three-dimensional time-harmonic Maxwell equations discretized by low order DG methods.

In the second order formulation of Maxwell's equation, the classical Schwarz method uses the impedance condition

$$\tilde{\mathcal{B}}_{\mathbf{n}}(\mathbf{E}) = (\nabla \times E \times \mathbf{n}) \times \mathbf{n} + i\tilde{\omega}\mathbf{E} \times \mathbf{n}, \tag{3.6}$$

see [11]. This impedance condition is equivalent to using the condition

$$\tilde{\mathcal{B}}_{\mathbf{n}}(\mathbf{E}) = (\nabla \times E \times \mathbf{n}) - i\tilde{\omega}\mathbf{n} \times (\mathbf{E} \times \mathbf{n}), \tag{3.7}$$

which is just a rotation by 90 degrees of (3.6), but is more adapted to variational formulations, see for example [5]. Condition (3.7) is equivalent to (3.5) if we replace $\mathbf{H}$ from Maxwell's equation as a function of $\nabla \times \mathbf{E}$. The equivalence between the first and second order formulation has been illustrated in [13] and [14].

As in (3.4), we also have the equivalences

$$\begin{aligned} &(G_{\mathbf{n}}^{-} + S_1 G_{\mathbf{n}}^{+})\mathbf{W}_1^{n+1} = (G_{\mathbf{n}}^{-} + S_1 G_{\mathbf{n}}^{+})\mathbf{W}_2^{n} \\ &\quad \Longleftrightarrow \quad (\mathcal{B}_{\mathbf{n}} + \tilde{S}_1\mathcal{B}_{-\mathbf{n}})(\mathbf{E}_1^{n+1}, \mathbf{H}_1^{n+1}) = (\mathcal{B}_{\mathbf{n}} + \tilde{S}_1\mathcal{B}_{-\mathbf{n}})(\mathbf{E}_2^{n}, \mathbf{H}_2^{n}), \\ &(G_{\mathbf{n}}^{+} + S_2 G_{\mathbf{n}}^{-})\mathbf{W}_2^{n+1} = (G_{\mathbf{n}}^{+} + S_2 G_{\mathbf{n}}^{-})\mathbf{W}_1^{n} \\ &\quad \Longleftrightarrow \quad (\mathcal{B}_{-\mathbf{n}} + \tilde{S}_2\mathcal{B}_{\mathbf{n}})(\mathbf{E}_2^{n+1}, \mathbf{H}_2^{n+1}) = (\mathcal{B}_{-\mathbf{n}} + \tilde{S}_2\mathcal{B}_{\mathbf{n}})(\mathbf{E}_1^{n}, \mathbf{H}_1^{n}). \end{aligned} \tag{3.8}$$

Here $\tilde{S}_1$ and $\tilde{S}_2$ denote differential operators which are approximations of the transparent operators and S_1 and S_2 are defined to guarantee the above equivalence. In [18], an entire hierarchy of optimized algorithms, defined by the choice of $\tilde{S}_j$, $j = 1, 2$, was obtained from the transparent operators. Using (3.2) and (3.3), the optimized transmission conditions (3.8) become

$$\begin{aligned} &N_{\mathbf{n}}N_{\mathbf{n}}^T\mathbf{E}_1^{n+1} - N_{\mathbf{n}}\mathbf{H}_1^{n+1} + \tilde{S}_1(N_{\mathbf{n}}N_{\mathbf{n}}^T\mathbf{E}_1^{n+1} + N_{\mathbf{n}}\mathbf{H}_1^{n+1}) \\ &\qquad = N_{\mathbf{n}}N_{\mathbf{n}}^T\mathbf{E}_2^{n} - N_{\mathbf{n}}\mathbf{H}_2^{n} + \tilde{S}_1(N_{\mathbf{n}}N_{\mathbf{n}}^T\mathbf{E}_2^{n} + N_{\mathbf{n}}\mathbf{H}_2^{n}), \\ &N_{\mathbf{n}}N_{\mathbf{n}}^T\mathbf{E}_2^{n+1} + N_{\mathbf{n}}\mathbf{H}_2^{n+1} + \tilde{S}_2(N_{\mathbf{n}}N_{\mathbf{n}}^T\mathbf{E}_2^{n+1} - N_{\mathbf{n}}\mathbf{H}_2^{n+1}) \\ &\qquad = N_{\mathbf{n}}N_{\mathbf{n}}^T\mathbf{E}_1^{n} + N_{\mathbf{n}}\mathbf{H}_1^{n} + \tilde{S}_2(N_{\mathbf{n}}N_{\mathbf{n}}^T\mathbf{E}_1^{n} - N_{\mathbf{n}}\mathbf{H}_1^{n}). \end{aligned} \tag{3.9}$$

4. Discontinuous Galerkin approximation. We now present a weak formulation and a DG discretization of the Schwarz algorithms (3.1), and show how optimized transmission conditions are properly discretized in a DG framework.

4.1. Weak Formulation. We denote by $\mathcal{T}_h$ a triangulation of the domain Ω, by Γ^0, Γ^m and Γ^a the sets of purely internal, metallic and absorbing faces, by K an element of $\mathcal{T}_h$ and by $F = K \cap \tilde{K}$ the face shared by two neighboring elements K and $\tilde{K}$. On each face F, we define the *average* $\{\mathbf{W}\}$ and the *tangential trace jump* $[\![\mathbf{W}]\!]$ of $\mathbf{W}$ by

$$\{\mathbf{W}\} := \frac{1}{2}(\mathbf{W}_K + \mathbf{W}_{\tilde{K}}) \quad \text{and} \quad [\![\mathbf{W}]\!] := G_{\mathbf{n}_K}\mathbf{W}_K + G_{\mathbf{n}_{\tilde{K}}}\mathbf{W}_{\tilde{K}}.$$

For two vector valued functions $\mathbf{U}$ and $\mathbf{V}$ in $(L^2(D))^6$, we denote by

$$(\mathbf{U},\mathbf{V})_D := \int_D \mathbf{U}\cdot\overline{\mathbf{V}}\,\mathrm{d}x,$$

if D is a domain of $\mathbb{R}^3$, and by

$$\langle \mathbf{U},\mathbf{V}\rangle_F = \int_F \mathbf{U}\cdot\overline{\mathbf{V}}\,\mathrm{d}s,$$

if F is a two-dimensional face. For simplicity, we will skip the index for $\mathcal{T}_h$, i.e. we write in what follows

$$(\cdot,\cdot) := (\cdot,\cdot)_{\mathcal{T}_h} = \sum_{K\in\mathcal{T}_h} (\cdot,\cdot)_K.$$

On the boundaries we define

$$M_{F,K} := \begin{cases} \begin{pmatrix} \eta_F N_{\mathbf{n}_K} N_{\mathbf{n}_K}^T & N_{\mathbf{n}_K} \\ -N_{\mathbf{n}_K}^T & 0_{3\times 3} \end{pmatrix} \text{ with } \eta_F \neq 0, \text{ if } F \text{ belongs to } \Gamma^m, \\ |G_{\mathbf{n}_K}| \text{ if } F \text{ belongs to } \Gamma^a. \end{cases}$$

We thus obtain a weak formulation of the problem,

$$\begin{aligned} (G_0\mathbf{W},\mathbf{V}) + \left(\sum_{l\in\{x,y,z\}} G_l\partial_l\mathbf{W},\mathbf{V}\right) - \sum_{F\in\Gamma^0}\langle[\![\mathbf{W}]\!],\{\mathbf{V}\}\rangle_F + \sum_{F\in\Gamma^0}\left\langle\frac{1}{2}[\![\mathbf{W}]\!],[\![\mathbf{V}]\!]\right\rangle_F \\ + \sum_{F\in\Gamma^m\cup\Gamma^a}\left\langle\frac{1}{2}(M_{F,K}-G_{\mathbf{n}_K})\mathbf{W},\mathbf{V}\right\rangle_F = \sum_{F\in\Gamma^a}\left\langle\frac{1}{2}(M_{F,K}-G_{\mathbf{n}_K})\mathbf{W}_{\mathrm{inc}},\mathbf{V}\right\rangle_F. \end{aligned} \tag{4.1}$$

4.2. Discretization of the Subdomain Problems and Classical Schwarz Algorithm. Let $\mathbb{P}_p(D)$ denote the space of polynomial functions of degree at most p on a domain D. For any element $K \in \mathcal{T}_h$, let $\mathbf{D}^p(K) \equiv (\mathbb{P}_p(K))^6$. The discontinuous finite element spaces we use are then defined by

$$\mathbf{D}_h^p = \left\{\mathbf{V}\in(L^2(\Omega))^6 \mid \mathbf{V}|_K \in \mathbf{D}^p(K),\ \forall K\in\mathcal{T}_h\right\}.$$

Approximate solutions $\mathbf{W}$ and test functions $\mathbf{V}$ for the discretized problem will be taken in the space $\mathbf{D}_h^p$.

Let Γ_Σ be the set of faces on the interface Σ, Γ_0^j be the set of faces in the interior of each subdomain Ω_j, and Γ_b^j be the set of faces for each subdomain which lie on the real boundary $\partial\Omega$. For any face $F = K \cap \tilde{K}$, note also that $G^2_{\mathbf{n}_K} = G^2_{\mathbf{n}_{\tilde{K}}} = |G_{\mathbf{n}_K}| = |G_{\mathbf{n}_{\tilde{K}}}|$.

Then for each subdomain Ω_1 and Ω_2, the weak form can be written as

$$\begin{aligned}
(G_0\mathbf{W}_1, \mathbf{V}_1) &+ \left(\sum_l G_l \partial_l \mathbf{W}_1, \mathbf{V}_1\right) + \sum_{\Gamma_0^1} \diamond + \sum_{\Gamma_b^1} \diamond \\
&+ \sum_{F\in\Gamma_\Sigma} \left\langle \frac{1}{2}\left(|G_{\mathbf{n}_K}| - G_{\mathbf{n}_K}\right)(\mathbf{W}_1 - \mathbf{W}_2), \mathbf{V}_1 \right\rangle_F = 0, \\
(G_0\mathbf{W}_2, \mathbf{V}_2) &+ \left(\sum_l G_l \partial_l \mathbf{W}_2, \mathbf{V}_2\right) + \sum_{\Gamma_0^2} \diamond + \sum_{\Gamma_b^2} \diamond \\
&+ \sum_{F\in\Gamma_\Sigma} \left\langle \frac{1}{2}\left(|G_{\mathbf{n}_{\tilde{K}}}| - G_{\mathbf{n}_{\tilde{K}}}\right)(\mathbf{W}_2 - \mathbf{W}_1), \mathbf{V}_2 \right\rangle_F = 0,
\end{aligned} \tag{4.2}$$

where, for simplicity, we have replaced some terms on the faces that do not play any particular role in what follows by a $\diamond$. For any face $F = K \cap \tilde{K}$ on Σ, if $\mathbf{n}$ denotes the normal on Σ directed from Ω_1 towards Ω_2, and K and $\tilde{K}$ are elements of Ω_1 and Ω_2, we have $\mathbf{n}_K = \mathbf{n} = -\mathbf{n}_{\tilde{K}}$.

The classical algorithm, which uses characteristic transmission conditions, corresponds in this DG formulation to a simple relaxation of the coupling flux terms in the coupled formulation (4.2): starting from initial guesses $\mathbf{W}_1^0$ and $\mathbf{W}_2^0$, it computes the iterates $\mathbf{W}_j^{n+1}$ from $\mathbf{W}_j^n$, $j = 1, 2$ by solving on Ω_1 and Ω_2 the subproblems

$$\begin{aligned}
\left(G_0\mathbf{W}_1^{n+1}, \mathbf{V}_1\right) &+ \left(\sum_l G_l \partial_l \mathbf{W}_1^{n+1}, \mathbf{V}_1\right) + \sum_{\Gamma_0^1} \diamond + \sum_{\Gamma_b^1} \diamond \\
&+ \sum_{F\in\Gamma_\Sigma} \left\langle G_{\mathbf{n}}^-(\mathbf{W}_1^{n+1} - \mathbf{W}_2^n), \mathbf{V}_1 \right\rangle_F = 0, \\
\left(G_0\mathbf{W}_2^{n+1}, \mathbf{V}_2\right) &+ \left(\sum_l G_l \partial_l \mathbf{W}_2^{n+1}, \mathbf{V}_2\right) + \sum_{\Gamma_0^2} \diamond + \sum_{\Gamma_b^2} \diamond \\
&+ \sum_{F\in\Gamma_\Sigma} \left\langle G_{\mathbf{n}}^+(\mathbf{W}_2^{n+1} - \mathbf{W}_1^n), \mathbf{V}_2 \right\rangle_F = 0,
\end{aligned} \tag{4.3}$$

where we used again (2.6) to simplify the notation. The relaxation in (4.3) is completely natural in the context of a DG discretization: we simply replaced the occurrence of the flux $G_{\mathbf{n}}^-\mathbf{W}_1^{n+1}$ from outside the subdomain by the flux from the neighboring subdomain $G_{\mathbf{n}}^-\mathbf{W}_2^n$ at the previous iteration, and vice versa, the occurrence of $G_{\mathbf{n}}^+\mathbf{W}_2^{n+1}$ by $G_{\mathbf{n}}^+\mathbf{W}_1^n$. This corresponds precisely to using the transmission conditions in (3.1) with $S_j = 0$, $j = 1, 2$, namely

$$\begin{aligned}
G_{\mathbf{n}}^-\mathbf{W}_1^{n+1} &= G_{\mathbf{n}}^-\mathbf{W}_2^n \\
G_{\mathbf{n}}^+\mathbf{W}_2^{n+1} &= G_{\mathbf{n}}^+\mathbf{W}_1^n,
\end{aligned} \tag{4.4}$$

and thus naturally guarantees at convergence of the associated classical Schwarz algorithm that the mono-domain DG solution is obtained. Such a simple replacement is however not possible for optimized transmission conditions, $S_j \neq 0$, and the dangerously naturally seeming DG discretization of the transmission conditions using the

variables available in each subdomain, namely

$$\begin{aligned} G_{\mathbf{n}}^{-}\mathbf{W}_1^{n+1} + S_1 G_{\mathbf{n}}^{+}\mathbf{W}_1^{n+1} &= G_{\mathbf{n}}^{-}\mathbf{W}_2^{n} + S_1 G_{\mathbf{n}}^{+}\mathbf{W}_2^{n}, \\ G_{\mathbf{n}}^{+}\mathbf{W}_2^{n+1} + S_2 G_{\mathbf{n}}^{-}\mathbf{W}_2^{n+1} &= G_{\mathbf{n}}^{+}\mathbf{W}_1^{n} + S_2 G_{\mathbf{n}}^{-}\mathbf{W}_1^{n}, \end{aligned} \tag{4.5}$$

leads to a DG solution obtained at convergence of the Schwarz algorithm which is different from the mono-domain DG solution, and thus for this different solution none of the DG error estimates hold. The solver should however never change the solution sought, and such a discretization is therefore to be avoided. We show in the next section how to properly discretize optimized transmission conditions in the framework of DG discretizations.

4.3. Discretization of Optimized Transmission Conditions. In order to correctly introduce optimized transmission conditions (3.1) with non-zero S_j into the DG discretization, we first write explicitly what transmission conditions the classical relaxation in (4.3) corresponds to. To do so, the subdomain problems solved in (4.3) are not allowed to depend on variables of the other subdomain anymore, since the coupling will be performed with the transmission conditions, and we thus need to introduce additional unknowns, namely $\mathbf{W}_{2,\Omega_1}^{n+1}$ on Ω_1 and $\mathbf{W}_{1,\Omega_2}^{n+1}$ on Ω_2, in order to write the classical Schwarz iteration with local variables only, *i.e.*

$$\begin{aligned} \big(G_0\mathbf{W}_1^{n+1}, \mathbf{V}_1\big) + \left(\sum_l G_l \partial_l \mathbf{W}_1^{n+1}, \mathbf{V}_1\right) + \sum_{\Gamma_0^1} \diamond + \sum_{\Gamma_b^1} \diamond \\ - \sum_{F\in\Gamma_\Sigma} \Big\langle G_{\mathbf{n}}^{-}(\mathbf{W}_1^{n+1} - \mathbf{W}_{2,\Omega_1}^{n+1}), \mathbf{V}_1 \Big\rangle_F = 0, \\ \big(G_0\mathbf{W}_2^{n+1}, \mathbf{V}_2\big) + \left(\sum_l G_l \partial_l \mathbf{W}_2^{n+1}, \mathbf{V}_2\right) + \sum_{\Gamma_0^2} \diamond + \sum_{\Gamma_b^2} \diamond \\ + \sum_{F\in\Gamma_\Sigma} \Big\langle G_{\mathbf{n}}^{+}(\mathbf{W}_2^{n+1} - \mathbf{W}_{1,\Omega_2}^{n+1}), \mathbf{V}_2 \Big\rangle_F = 0. \end{aligned} \tag{4.6}$$

Comparing with the classical Schwarz algorithm (4.3), we see that in order to obtain the same algorithm, the transmission conditions for (4.6) need to be chosen as

$$G_{\mathbf{n}}^{-}\mathbf{W}_{2,\Omega_1}^{n+1} = G_{\mathbf{n}}^{-}\mathbf{W}_2^{n}, \qquad G_{\mathbf{n}}^{+}\mathbf{W}_{1,\Omega_2}^{n+1} = G_{\mathbf{n}}^{+}\mathbf{W}_1^{n}, \tag{4.7}$$

which we have already seen when explicitly stating the relaxation as a replacement in (4.4). But one has to be careful when keeping these variables, since they represent the outside traces at the interface, not the inside traces of the elements! The transmission condition (4.7) implies that in the limit, when the algorithm converges, the so called *coupling conditions*

$$G_{\mathbf{n}}^{-}\mathbf{W}_{2,\Omega_1} = G_{\mathbf{n}}^{-}\mathbf{W}_2, \qquad G_{\mathbf{n}}^{+}\mathbf{W}_{1,\Omega_2} = G_{\mathbf{n}}^{+}\mathbf{W}_1, \tag{4.8}$$

will be verified, where we dropped the iteration index to denote the limit quantities. These are the conditions which imply the same converged solution as the mono-domain DG solution. When using the Schwarz algorithm (4.6) with optimized transmission conditions (3.1), we therefore propose to use DG discretizations of the strong relations

$$\begin{aligned} G_{\mathbf{n}}^{-}\mathbf{W}_{2,\Omega_1}^{n+1} + S_1 G_{\mathbf{n}}^{+}\mathbf{W}_1^{n+1} &= G_{\mathbf{n}}^{-}\mathbf{W}_2^{n} + S_1 G_{\mathbf{n}}^{+}\mathbf{W}_{1,\Omega_2}^{n}, \\ G_{\mathbf{n}}^{+}\mathbf{W}_{1,\Omega_2}^{n+1} + S_2 G_{\mathbf{n}}^{-}\mathbf{W}_2^{n+1} &= G_{\mathbf{n}}^{+}\mathbf{W}_1^{n} + S_2 G_{\mathbf{n}}^{-}\mathbf{W}_{2,\Omega_1}^{n}, \end{aligned} \tag{4.9}$$

which are substantially different from the transmission conditions (4.5), since they use additional variables $\mathbf{W}_{2,\Omega_1}$ and $\mathbf{W}_{1,\Omega_2}$ which in principle belong to the traces at the interface Σ of the neighboring subdomain, and are not available in the formulation (4.5). We will now prove that with the transmission conditions (4.9), at convergence of the associated Schwarz algorithm the same coupling conditions as (4.8) hold, and thus the optimized Schwarz method converges to the mono-domain solution of the DG discretization chosen. First, from (3.2) and (3.3), note that relation (4.8) is equivalent to

$$\begin{cases} N_{\mathbf{n}} N_{\mathbf{n}}^T \mathbf{E}_{2,\Omega_1} - N_{\mathbf{n}} \mathbf{H}_{2,\Omega_1} = N_{\mathbf{n}} N_{\mathbf{n}}^T \mathbf{E}_2 - N_{\mathbf{n}} \mathbf{H}_2, \\ N_{\mathbf{n}} N_{\mathbf{n}}^T \mathbf{E}_{1,\Omega_2} + N_{\mathbf{n}} \mathbf{H}_{1,\Omega_2} = N_{\mathbf{n}} N_{\mathbf{n}}^T \mathbf{E}_1 + N_{\mathbf{n}} \mathbf{H}_1. \end{cases} \tag{4.10}$$

We now introduce the auxiliary variables

$$\begin{array}{ll} \Lambda_{2,\Omega_1} := N_{\mathbf{n}} N_{\mathbf{n}}^T \mathbf{E}_{2,\Omega_1} - N_{\mathbf{n}} \mathbf{H}_{2,\Omega_1}, & \Lambda_2 := N_{\mathbf{n}} N_{\mathbf{n}}^T \mathbf{E}_2 - N_{\mathbf{n}} \mathbf{H}_2, \\ \Lambda_{1,\Omega_2} := N_{\mathbf{n}} N_{\mathbf{n}}^T \mathbf{E}_{1,\Omega_2} + N_{\mathbf{n}} \mathbf{H}_{1,\Omega_2}, & \Lambda_1 := N_{\mathbf{n}} N_{\mathbf{n}}^T \mathbf{E}_1 + N_{\mathbf{n}} \mathbf{H}_1. \end{array} \tag{4.11}$$

These variables represent traces belonging to a traced finite-element space

$$M_h^p = \left\{ \boldsymbol{\eta} \in (L^2(\Sigma))^3 \mid \boldsymbol{\eta}|_F \in (\mathbb{P}_p(F))^3,\ (\boldsymbol{\eta} \cdot \mathbf{n})|_F = 0,\ \forall F \in \Sigma \right\}. \tag{4.12}$$

Note that M_h^p consists of vector-valued functions whose normal component is zero on any face $F \in \Sigma$. At convergence of the classical Schwarz algorithm, and hence for the mono-domain DG solution, we see from (4.8) that these trace variables have to satisfy

$$\Lambda_{2,\Omega_1} = \Lambda_2, \qquad \Lambda_{1,\Omega_2} = \Lambda_1. \tag{4.13}$$

From (4.9) and (4.13), we have to find for optimized transmission conditions a suitable DG discretization of the relations

$$\Lambda_{2,\Omega_1} + \tilde{S}_1 \Lambda_1 = \Lambda_2 + \tilde{S}_1 \Lambda_{1,\Omega_2}, \qquad \Lambda_{1,\Omega_2} + \tilde{S}_2 \Lambda_2 = \Lambda_1 + \tilde{S}_2 \Lambda_{2,\Omega_1}. \tag{4.14}$$

In [18], it was shown that the optimized operators $\tilde{S}_j$, $j = 1, 2$, are second order operators (see Table 4.1) where

$$\tilde{Q}_{s_j} = \begin{bmatrix} \partial_{\tau_1\tau_1} - \partial_{\tau_2\tau_2} - \tilde{\sigma} s_j & 2\partial_{\tau_1\tau_2} \\ 2\partial_{\tau_1\tau_2} & \partial_{\tau_2\tau_2} - \partial_{\tau_1\tau_1} - \tilde{\sigma} s_j \end{bmatrix},$$

and the division by $|\mathbf{k}|^2$ indicates an integral operation. Note that the operator $\tilde{Q}_{s_j}$ can be re-written as

$$\begin{aligned} \tilde{Q}_{s_j} &= \begin{bmatrix} \partial_{\tau_1\tau_1} & \partial_{\tau_1\tau_2} \\ \partial_{\tau_1\tau_2} & \partial_{\tau_2\tau_2} \end{bmatrix} + \begin{bmatrix} -\partial_{\tau_2\tau_2} & \partial_{\tau_1\tau_2} \\ \partial_{\tau_1\tau_2} & -\partial_{\tau_1\tau_1} \end{bmatrix} - \tilde{\sigma} s_j Id \\ &= \underbrace{\nabla_\tau \nabla_\tau \cdot}_{\mathcal{S}_{TM}} + \underbrace{\nabla_\tau \times \nabla_\tau \times}_{\mathcal{S}_{TE}} - \tilde{\sigma} s_j Id, \end{aligned}$$

where Id denotes the identity operator, τ_j, $j = 1, 2$ are two independent vectors in the tangent plane to the interface, ∇_τ denotes the gradient in the tangent plane to the interface, $\nabla_\tau \cdot$ is the divergence in the tangent plane and $\nabla_\tau \times$ is the two-dimensional curl operator in the tangent plane. The operators $\mathcal{S}_{TM}$ and $\mathcal{S}_{TE}$ verify the remarkable relation

$$-\Delta_\tau Id = \mathcal{S}_{TE} - \mathcal{S}_{TM},$$

Algorithm	$\mathcal{F}(\tilde{S}_j)$
1	0
2	$\frac{s-i\tilde{\omega}}{(s+i\tilde{\omega})(\lvert\mathbf{k}\rvert^2+s\tilde{\sigma})}\mathcal{F}(\tilde{Q}_s), \qquad s\in\mathbb{C}$
3	$\frac{1}{\lvert\mathbf{k}\rvert^2-2\tilde{\omega}^2+2i\tilde{\omega}\tilde{\sigma}+(2i\tilde{\omega}+\tilde{\sigma})s}\mathcal{F}(\tilde{Q}_s), \qquad s\in\mathbb{C}$
4	$\frac{s_j-i\tilde{\omega}}{(s_j+i\tilde{\omega})(\lvert\mathbf{k}\rvert^2+s_j\tilde{\sigma})}\mathcal{F}(\tilde{Q}_{s_j}), \quad s_j\in\mathbb{C}$
5	$\frac{1}{\lvert\mathbf{k}\rvert^2-2\tilde{\omega}^2+2i\tilde{\omega}\tilde{\sigma}+(2i\tilde{\omega}+\tilde{\sigma})s_j}\mathcal{F}(\tilde{Q}_{s_j}), \quad s_j\in\mathbb{C}$

Table 4.1: Symbols of the different operators

where Δ_τ is the Laplace-Beltrami operator, and they act mainly on the transverse electric and transverse magnetic part of the solution, see [13] and [14] for more details.

To avoid an integral relation in the transmission condition, one has to multiply the entire transmission conditions by the operator symbol in the denominator, and then obtains second order differential transmission conditions. These second order differential transmission conditions are equivalent to the transmission conditions (4.14), and are of the form

$$\begin{aligned}\tilde{P}_1(\Lambda_{2,\Omega_1}-\Lambda_2) &= \tilde{Q}_{s_1}(\Lambda_{1,\Omega_2}-\Lambda_1),\\ \tilde{P}_2(\Lambda_{1,\Omega_2}-\Lambda_1) &= \tilde{Q}_{s_2}(\Lambda_{2,\Omega_1}-\Lambda_2),\end{aligned} \tag{4.15}$$

where for example for the Algorithms 2 and 4 indicated in Table 4.1 we have

$$\tilde{P}_j := \frac{s_j+i\tilde{\omega}}{s_j-i\tilde{\omega}}(-\Delta_\tau+\tilde{\sigma}s_j)Id, \quad s_j\in\mathbb{C}, \tag{4.16}$$

and for the Algorithms 3 and 5 we have

$$\begin{aligned}\tilde{P}_j : &= (-\Delta_\tau-2\tilde{\omega}^2+2i\tilde{\omega}\tilde{\sigma}+2i\tilde{\omega}s_j+\tilde{\sigma}s_j)Id\\ &= \mathcal{S}_{TE}-\mathcal{S}_{TM}+(-2\tilde{\omega}^2+2i\tilde{\omega}\tilde{\sigma}+2i\tilde{\omega}s_j+\tilde{\sigma}s_j)Id, \quad s_j\in\mathbb{C}.\end{aligned} \tag{4.17}$$

Here the parameters s_j, $j=1,2$ can be chosen to optimize the performance of the method, see Table 4.2 for asymptotically optimized values.

Let $(\boldsymbol{\eta}_j)_j$ be a basis of M_h^p. We define on the interface Σ the matrices

$$(M_\Sigma)_{i,j} := \sum_{F\in\Sigma}\langle\boldsymbol{\eta}_i,\boldsymbol{\eta}_j\rangle_F,$$

$$\begin{aligned}(K_\Sigma)_{i,j} := &\sum_{F\in\Sigma}\langle\nabla_\tau\times\boldsymbol{\eta}_i,\nabla_\tau\times\boldsymbol{\eta}_j\rangle_F+\langle\nabla_\tau\cdot\boldsymbol{\eta}_i,\nabla_\tau\cdot\boldsymbol{\eta}_j\rangle_F\\ &+\sum_{e\in\partial\Sigma}\int_e\alpha h^{-1}\sum_{k\in\{1,2\}}[\![[\boldsymbol{\eta}_i\cdot\tau_k]\!][\![[\boldsymbol{\eta}_j\cdot\tau_k]\!]\\ &-\sum_{e\in\partial\Sigma}\int_e\{\{\nabla_\tau\cdot\boldsymbol{\eta}_i\}\}[\![[\boldsymbol{\eta}_j\cdot n_{e,\tau}]\!]-[\![[\boldsymbol{\eta}_i\cdot n_{e,\tau}]\!]\{\{\nabla_\tau\cdot\boldsymbol{\eta}_j\}\}\\ &-\sum_{e\in\partial\Sigma}\int_e\{\{\nabla_\tau\times\boldsymbol{\eta}_i\}\}\cdot[\![[\boldsymbol{\eta}_j\times n_{e,\tau}]\!]-[\![[\boldsymbol{\eta}_i\times n_{e,\tau}]\!]\cdot\{\{\nabla_\tau\times\boldsymbol{\eta}_j\}\},\end{aligned}$$

	with overlap, $L = h$	
Algorithm	ρ	parameters
1	$1 - \frac{4}{3}\left(9\tilde{\omega}^4\tilde{\sigma}^2\right)^{\frac{1}{8}} h^{\frac{3}{4}}$	none
2	$1 - 2^{\frac{7}{6}} \left(\tilde{\omega}\,\tilde{\sigma}\right)^{1/6} h^{\frac{1}{3}}$	$p = \frac{(2\,\tilde{\omega}\,\tilde{\sigma})^{1/3}}{2\,h^{\frac{1}{3}}}$
3	$1 - \frac{2^{\frac{17}{10}} (\tilde{\omega}^4\tilde{\sigma}^2)^{\frac{1}{20}} h^{\frac{3}{10}}}{3^{\frac{3}{10}}}$	$p = \frac{2^{\frac{2}{5}} (\tilde{\omega}^4\tilde{\sigma}^2)^{\frac{1}{10}}}{3^{\frac{3}{5}} h^{\frac{2}{5}}}$
4	$1 - 4\sqrt{2} \left(\tilde{\omega}\,\tilde{\sigma}\right)^{\frac{1}{10}} h^{\frac{1}{5}}$	$p_1 = \frac{(\tilde{\omega}\,\tilde{\sigma})^{\frac{1}{5}}}{2\,h^{\frac{3}{5}}}$, $p_2 = \frac{(\tilde{\omega}\,\tilde{\sigma})^{\frac{2}{5}}}{2\,h^{\frac{1}{5}}}$
5	$1 - \frac{2^{\frac{23}{8}} (\tilde{\omega}^4\tilde{\sigma}^2)^{\frac{1}{32}} h^{\frac{3}{16}}}{3^{\frac{3}{16}}}$	$p_1 = \frac{(\tilde{\omega}^4\tilde{\sigma}^2)^{\frac{1}{16}}}{2^{\frac{1}{4}} 3^{\frac{3}{8}} h^{\frac{5}{8}}}$,$p_2 = \frac{\sqrt{2}(\tilde{\omega}^4\tilde{\sigma}^2)^{\frac{1}{8}}}{3^{\frac{3}{4}} h^{\frac{1}{4}}}$
	without overlap, $L = 0$	
1	$1 - \frac{\tilde{\omega}^2\tilde{\sigma}}{C^3} h^3$	none
2	$1 - \frac{2^{\frac{3}{4}} (\tilde{\omega}\tilde{\sigma})^{\frac{1}{4}} \sqrt{h}}{\sqrt{C}}$	$p = \frac{(\tilde{\omega}\tilde{\sigma})^{\frac{1}{4}} \sqrt{C}}{2^{\frac{1}{4}} \sqrt{h}}$
3	$1 - \frac{2^{\frac{11}{7}} (\tilde{\omega}^4\tilde{\sigma}^2)^{\frac{1}{14}} h^{\frac{3}{7}}}{3^{\frac{3}{7}} C^{\frac{3}{7}}}$	$p = \frac{2^{\frac{4}{7}} (\tilde{\omega}^4\tilde{\sigma}^2)^{\frac{1}{14}} C^{\frac{4}{7}}}{3^{\frac{3}{7}} h^{\frac{4}{7}}}$
4	$1 - \frac{(2\,\tilde{\omega}\,\tilde{\sigma})^{\frac{1}{8}} h^{\frac{1}{4}}}{C^{\frac{1}{4}}}$	$p_1 = \frac{(2\,\tilde{\omega}\,\tilde{\sigma})^{\frac{1}{8}} C^{\frac{3}{4}}}{h^{\frac{3}{4}}}$, $p_2 = \frac{(2\,\tilde{\omega}\,\tilde{\sigma})^{3/8} C^{1/4}}{2\,h^{\frac{1}{4}}}$
5	$1 - \frac{2^{\frac{34}{13}} (\tilde{\omega}^4\tilde{\sigma}^2)^{\frac{1}{26}} h^{\frac{3}{13}}}{3^{\frac{3}{13}} C^{\frac{3}{13}}}$	$p_1 = \frac{2^{\frac{8}{13}} (\tilde{\omega}^4\tilde{\sigma}^2)^{\frac{1}{26}} C^{\frac{10}{13}}}{3^{\frac{3}{13}} h^{\frac{10}{13}}}$,$p_2 = \frac{2^{\frac{11}{13}} (\tilde{\omega}^4\tilde{\sigma}^2)^{\frac{3}{26}} C^{\frac{4}{13}}}{3^{\frac{9}{13}} h^{\frac{4}{13}}}$

Table 4.2: Asymptotic convergence factor and optimal choice of the parameters in the transmission conditions.

and

$$
\begin{aligned}
(A_\Sigma)_{i,j} := & \sum_{F\in\Sigma} \langle \nabla_\tau \times \boldsymbol{\eta}_i, \nabla_\tau \times \boldsymbol{\eta}_j \rangle_F - \langle \nabla_\tau \cdot \boldsymbol{\eta}_i, \nabla_\tau \cdot \boldsymbol{\eta}_j \rangle_F \\
& + \sum_{e\in\partial\Sigma} \int_e \alpha h^{-1} \sum_{k\in\{1,2\}} [\![[\![\boldsymbol{\eta}_i \cdot \tau_k]\!] [\![\boldsymbol{\eta}_j \cdot \tau_k]\!]]\!] \\
& + \sum_{e\in\partial\Sigma} \int_e \{\{\nabla_\tau \cdot \boldsymbol{\eta}_i\}\} [\![[\![\boldsymbol{\eta}_j \cdot n_{e,\tau}]\!]]\!] - [\![[\![\boldsymbol{\eta}_i \cdot n_{e,\tau}]\!]]\!] \{\{\nabla_\tau \cdot \boldsymbol{\eta}_j\}\}, \\
& - \sum_{e\in\partial\Sigma} \int_e \{\{\nabla_\tau \times \boldsymbol{\eta}_i\}\} \cdot [\![[\![\boldsymbol{\eta}_j \times n_{e,\tau}]\!]]\!] - [\![[\![\boldsymbol{\eta}_i \times n_{e,\tau}]\!]]\!] \cdot \{\{\nabla_\tau \times \boldsymbol{\eta}_j\}\},
\end{aligned}
$$

where the positivity of the discretized operator is guaranteed for sufficiently large α, $\partial\Sigma$ denotes the set of interior edges of Σ, $[\![\cdot]\!]$ and $\{\{\cdot\}\}$ denote the jump and the average at an edge e between values of the neighboring triangles, and $n_{e,\tau}$ is the outward normal on e in the tangent plane. Then matrix K_Σ comes from the discretization of $-\Delta_\tau$ using a symmetric interior penalty approach [3, 2]. Note that the $-\Delta_\tau$ operator has to be taken in "vector" form, since it is applied to $(\Lambda_{2,\tilde{\Omega}_1} - \Lambda_2)$, which is a discretization of a vector quantity. M_Σ is an interface mass matrix with the same dimensions as the interface stiffness matrix K_Σ, and A_Σ represents the discretization of the operator

$$
\begin{bmatrix} \partial_{\tau_1\tau_1} - \partial_{\tau_2\tau_2} & 2\partial_{\tau_1\tau_2} \\ 2\partial_{\tau_1\tau_2} & \partial_{\tau_2\tau_2} - \partial_{\tau_1\tau_1} \end{bmatrix}.
$$

Then the DG discretization of (4.15) for the Algorithms 2 and 4 is

$$\begin{aligned}\frac{s_1+i\tilde{\omega}}{s_1-i\tilde{\omega}}(K_\Sigma+\tilde{\sigma}s_1M_\Sigma)(\Lambda_{2,\Omega_1}-\Lambda_2)&=(A_\Sigma-\tilde{\sigma}s_1M_\Sigma)(\Lambda_{1,\Omega_2}-\Lambda_1),\\ \frac{s_2+i\tilde{\omega}}{s_2-i\tilde{\omega}}(K_\Sigma+\tilde{\sigma}s_2M_\Sigma)(\Lambda_{1,\Omega_2}-\Lambda_1)&=(A_\Sigma-\tilde{\sigma}s_2M_\Sigma)(\Lambda_{2,\Omega_1}-\Lambda_2),\end{aligned} \tag{4.18}$$

and for the Algorithms 3 and 5 we get

$$\begin{aligned}(K_\Sigma+\alpha_1M_\Sigma)(\Lambda_{2,\Omega_1}-\Lambda_2)&=(A_\Sigma-\tilde{\sigma}s_1M_\Sigma)(\Lambda_{1,\Omega_2}-\Lambda_1),\\ (K_\Sigma+\alpha_2M_\Sigma)(\Lambda_{1,\Omega_2}-\Lambda_1)&=(A_\Sigma-\tilde{\sigma}s_2M_\Sigma)(\Lambda_{2,\Omega_1}-\Lambda_2),\end{aligned} \tag{4.19}$$

where $\alpha_j=2i\tilde{\omega}(i\tilde{\omega}+\tilde{\sigma})+2i\tilde{\omega}s_j+\tilde{\sigma}s_j$. In the following theorem we will only treat the case of Algorithms 3 and 5, similar techniques can be applied for Algorithms 2 and 4.

THEOREM 4.1 (DG discretization of Algorithms 3 and 5). *If s_1 and s_2 are such that $s_j=p_j(1+i)$ with p_j a strictly positive real number for $j=1,2$, and $\tilde{\sigma}(p_1-p_2)=0$, then the relations* (4.13) *and* (4.19) *are equivalent.*

Proof. We first see that $\Im\alpha_j=2\tilde{\omega}\tilde{\sigma}+2\tilde{\omega}p_j+\tilde{\sigma}p_j>0$. Let us denote by

$$\mathbf{U}_1=\Lambda_{1,\Omega_2}-\Lambda_1,\quad \mathbf{U}_2=\Lambda_{2,\Omega_1}-\Lambda_2.$$

Multiplying the first relation in (4.19) on the left by $\bar{\mathbf{U}}_2^T$ and the second by $\bar{\mathbf{U}}_1^T$ and summing them, we get

$$\bar{\mathbf{U}}_2^T(K_\Sigma+\alpha_1M_\Sigma)\mathbf{U}_2+\bar{\mathbf{U}}_1^T(K_\Sigma+\alpha_2M_\Sigma)\mathbf{U}_1=\bar{\mathbf{U}}_2^T(A_\Sigma-\tilde{\sigma}s_1M_\Sigma)\mathbf{U}_1+\bar{\mathbf{U}}_1^T(A_\Sigma-\tilde{\sigma}s_2M_\Sigma)\mathbf{U}_2. \tag{4.20}$$

Since K_Σ is symmetric and non-negative, M_Σ is symmetric and positive definite, and A_Σ is symmetric, all the quantities $\bar{\mathbf{U}}_j^TM_\Sigma\mathbf{U}_j$, $\bar{\mathbf{U}}_j^TK_\Sigma\mathbf{U}_j$ and $\bar{\mathbf{U}}_1^TA_\Sigma\mathbf{U}_2+\bar{\mathbf{U}}_2^TA_\Sigma\mathbf{U}_1$ are real. In this case, by taking the imaginary part of the previous relation we get

$$\Im\alpha_1\bar{\mathbf{U}}_2^TM_\Sigma\mathbf{U}_2+\Im\alpha_2\bar{\mathbf{U}}_1^TM_\Sigma\mathbf{U}_1+\tilde{\sigma}\Im(s_1\bar{\mathbf{U}}_2^TM_\Sigma\mathbf{U}_1+s_2\bar{\mathbf{U}}_1^TM_\Sigma\mathbf{U}_2)=0. \tag{4.21}$$

In order to simplify the notation, using that M_Σ is symmetric positive definite, we introduce the norm $\|\mathbf{U}\|_{M_\Sigma}^2:=\bar{\mathbf{U}}^TM_\Sigma\mathbf{U}$, which is induced by the hermitian product $(\mathbf{U}_1,\mathbf{U}_2)_{M_\Sigma}=\bar{\mathbf{U}}_2^TM_\Sigma\mathbf{U}_1$. Since by definition $(\mathbf{U}_2,\mathbf{U}_1)_{M_\Sigma}=\overline{(\mathbf{U}_1,\mathbf{U}_2)}_{M_\Sigma}$, we see that

$$\begin{aligned}&\Im(\bar{\mathbf{U}}_2^TM_\Sigma\mathbf{U}_1)=\tfrac{1}{2i}((\mathbf{U}_1,\mathbf{U}_2)_{M_\Sigma}-(\mathbf{U}_2,\mathbf{U}_1)_{M_\Sigma})=-\Im(\bar{\mathbf{U}}_1^TM_\Sigma\mathbf{U}_2),\\ &\Re(\bar{\mathbf{U}}_2^TM_\Sigma\mathbf{U}_1)=\tfrac{1}{2}((\mathbf{U}_1,\mathbf{U}_2)_{M_\Sigma}+(\mathbf{U}_2,\mathbf{U}_1)_{M_\Sigma})=\Re(\bar{\mathbf{U}}_1^TM_\Sigma\mathbf{U}_2),\\ &\Im(s_1\bar{\mathbf{U}}_2^TM_\Sigma\mathbf{U}_1)=p_1(\Re(\mathbf{U}_1,\mathbf{U}_2)_{M_\Sigma}+\Im(\mathbf{U}_1,\mathbf{U}_2)_{M_\Sigma}),\\ &\Im(s_2\bar{\mathbf{U}}_1^TM_\Sigma\mathbf{U}_2)=p_2(\Re(\mathbf{U}_2,\mathbf{U}_1)_{M_\Sigma}+\Im(\mathbf{U}_2,\mathbf{U}_1)_{M_\Sigma})=p_2(\Re(\mathbf{U}_1,\mathbf{U}_2)_{M_\Sigma}-\Im(\mathbf{U}_1,\mathbf{U}_2)_{M_\Sigma}).\end{aligned}$$

Also let $p_1=p+\delta$ and $p_2=p-\delta$ and suppose $\delta\geqslant 0$. Then (4.21) becomes

$$\begin{aligned}&2\tilde{\omega}(\tilde{\sigma}+p_1)\|\mathbf{U}_2\|_{M_\Sigma}^2+2\tilde{\omega}(\tilde{\sigma}+p_2)\|\mathbf{U}_1\|_{M_\Sigma}^2+\tilde{\sigma}(p+\delta)\|\mathbf{U}_2\|_{M_\Sigma}^2+\tilde{\sigma}(p-\delta)\|\mathbf{U}_1\|_{M_\Sigma}^2\\ &\quad+\tilde{\sigma}(p+\delta)(\Re(\mathbf{U}_1,\mathbf{U}_2)_{M_\Sigma}+\Im(\mathbf{U}_1,\mathbf{U}_2)_{M_\Sigma})\\ &\quad+\tilde{\sigma}(p-\delta)(\Re(\mathbf{U}_1,\mathbf{U}_2)_{M_\Sigma}-\Im(\mathbf{U}_1,\mathbf{U}_2)_{M_\Sigma})=0\\ \Leftrightarrow\ &2\tilde{\omega}(\tilde{\sigma}+p_1)\|\mathbf{U}_2\|_{M_\Sigma}^2+2\tilde{\omega}(\tilde{\sigma}+p_2)\|\mathbf{U}_1\|_{M_\Sigma}^2\\ &\quad+\tilde{\sigma}p(\|\mathbf{U}_2\|_{M_\Sigma}^2+\|\mathbf{U}_1\|_{M_\Sigma}^2+2\Re(\mathbf{U}_1,\mathbf{U}_2)_{M_\Sigma})\\ &\quad+\tilde{\sigma}\delta(\|\mathbf{U}_2\|_{M_\Sigma}^2-\|\mathbf{U}_1\|_{M_\Sigma}^2+2\Im(\mathbf{U}_1,\mathbf{U}_2)_{M_\Sigma})=0,\\ \Leftrightarrow\ &2\tilde{\omega}(\tilde{\sigma}+p_1)\|\mathbf{U}_2\|_{M_\Sigma}^2+2\tilde{\omega}(\tilde{\sigma}+p_2)\|\mathbf{U}_1\|_{M_\Sigma}^2+\tilde{\sigma}p\|\mathbf{U}_1+\mathbf{U}_2\|_{M_\Sigma}^2\\ &\quad+\tilde{\sigma}\delta(\|\mathbf{U}_2\|_{M_\Sigma}^2-\|\mathbf{U}_1\|_{M_\Sigma}^2+2\Im(\mathbf{U}_1,\mathbf{U}_2)_{M_\Sigma})=0.\end{aligned} \tag{4.22}$$

We thus see that if $\tilde{\sigma}=0$ or $\delta=0$, which means $p_1=p_2$ (Algorithm 3 from Table 4.2), then the last form of (4.22) leads to the conclusion that $\mathbf{U}_j=0$, since all the terms are positive, which proves the equivalence between (4.19) and (4.13). ∎

4.4. Two-dimensional case. Like in the three-dimensional case, we can rewrite (4.9) and (4.8) by introducing the auxiliary variables (see [4] for more details)

$$\begin{array}{l} \Lambda_{2,\Omega_1} := E_{2,\Omega_1} - N_{\mathbf{n}}\mathbf{H}_{2,\Omega_1},\ \Lambda_2 := E_2 - N_{\mathbf{n}}\mathbf{H}_2, \\ \Lambda_{1,\Omega_2} := E_{1,\Omega_2} + N_{\mathbf{n}}\mathbf{H}_{1,\Omega_2},\ \Lambda_1 := E_1 + N_{\mathbf{n}}\mathbf{H}_1, \end{array} \tag{4.23}$$

belonging to the trace space $M_h^p = \left\{\eta \in L^2(\Sigma) \mid \eta|_F \in \mathbb{P}_p(F),\ \forall F \in \Sigma\right\}$. Then (4.8) becomes

$$\Lambda_{2,\Omega_1} = \Lambda_2 \ \text{ and } \ \Lambda_{1,\Omega_2} = \Lambda_1. \tag{4.24}$$

From (4.9) and (4.23), we see that we have to find for optimized transmission conditions a suitable DG discretization of the relations

$$\Lambda_{2,\Omega_1} + \tilde{S}_1\Lambda_1 = \Lambda_2 + \tilde{S}_1\Lambda_{1,\Omega_2} \ \text{ and } \ \Lambda_{1,\Omega_2} + \tilde{S}_2\Lambda_2 = \Lambda_1 + \tilde{S}_2\Lambda_{2,\Omega_1}. \tag{4.25}$$

If we focus on the second order transmission conditions, (4.25) becomes

$$\begin{array}{rcl} (-\partial_\tau^2 + i\tilde{\omega}\tilde{\sigma} - 2\tilde{\omega}^2 + 2i\tilde{\omega}s_1)(\Lambda_{2,\Omega_1} - \Lambda_2) + (-\partial_\tau^2 + i\tilde{\omega}\tilde{\sigma})(\Lambda_{1,\Omega_2} - \Lambda_1) & = & 0, \\ (-\partial_\tau^2 + i\tilde{\omega}\tilde{\sigma} - 2\tilde{\omega}^2 + 2i\tilde{\omega}s_2)(\Lambda_{1,\Omega_2} - \Lambda_1) + (-\partial_\tau^2 + i\tilde{\omega}\tilde{\sigma})(\Lambda_{2,\Omega_1} - \Lambda_2) & = & 0. \end{array} \tag{4.26}$$

Let $(\eta_j)_j$ be a basis of M_h^p. We define the matrices

$$\begin{array}{rcl} (M_\Sigma)_{i,j} & := & \displaystyle\sum_{F\in\Sigma} \langle \eta_i, \eta_j \rangle_F, \\ (K_\Sigma)_{i,j} & := & \displaystyle\sum_{F\in\Sigma} \langle \partial_\tau\eta_i, \partial_\tau\eta_j \rangle_F + \sum_{n\in\Sigma^0} \alpha_n h^{-1} [[[[\eta_i]]]]_n [[[[\eta_j]]]]_n \\ & - & \displaystyle\sum_{n\in\Sigma^0} \{\{\partial_\tau\eta_i\}\}_n [[[[\eta_j]]]]_n - [[[[\eta_i]]]]_n \{\{\partial_\tau\eta_j\}\}_n, \end{array}$$

where positiveness is guaranteed for sufficiently large α_n, Σ^0 denotes the set of interior nodes of Σ, $[[[[\cdot]]]]_n$ and $\{\{\cdot\}\}_n$ denotes the jump and the average at a node n between values of the neighboring segments. The matrix K_Σ comes from the discretization of $-\partial_\tau^2$ using a symmetric interior penalty approach [2].

The DG discretization of (4.26) is then

$$\begin{array}{l} (K_\Sigma + \alpha_1 M_\Sigma)(\Lambda_{2,\Omega_1} - \Lambda_2) = (-K_\Sigma - i\tilde{\omega}\tilde{\sigma}M_\Sigma)(\Lambda_{1,\Omega_2} - \Lambda_1), \\ (K_\Sigma + \alpha_2 M_\Sigma)(\Lambda_{1,\Omega_2} - \Lambda_1) = (-K_\Sigma - i\tilde{\omega}\tilde{\sigma}M_\Sigma)(\Lambda_{2,\Omega_1} - \Lambda_2), \end{array} \tag{4.27}$$

with $\alpha_j = -2\tilde{\omega}^2 + i(\tilde{\omega}\tilde{\sigma} + 2\tilde{\omega}p_j)$. As in the three-dimensional case, K_Σ is symmetric and non-negative definite, and M_Σ is symmetric and positive definite. A similar result to Theorem 4.1 can be obtained also in 2d:

THEOREM 4.2 (DG discretization for the second order conditions in 2d). *If s_1 and s_2 are such that $s_j = p_j(1+i)$ with p_j a strictly positive real number for $j = 1, 2$, then the relations* (4.24) *and* (4.27) *are equivalent.*

Proof. We first note that $\Im\alpha_j = \tilde{\omega}\tilde{\sigma} + 2\tilde{\omega}p_j > 0$. Setting

$$\mathbf{U}_1 = \Lambda_{1,\Omega_2} - \Lambda_1, \quad \mathbf{U}_2 = \Lambda_{2,\Omega_1} - \Lambda_2,$$

and multiplying the first relation in (4.27) on the left by $\bar{\mathbf{U}}_2^T$, the second by $\bar{\mathbf{U}}_1^T$, and adding them, we obtain by taking the imaginary part

$$(\tilde{\omega}\tilde{\sigma} + 2\tilde{\omega}p_j)(\bar{\mathbf{U}}_1^T M_\Sigma \mathbf{U}_1 + \bar{\mathbf{U}}_2^T M_\Sigma \mathbf{U}_2) = -\tilde{\omega}\tilde{\sigma}(\bar{\mathbf{U}}_2^T M_\Sigma \mathbf{U}_1 + \bar{\mathbf{U}}_1^T M_\Sigma \mathbf{U}_2)$$

By re-arranging the terms and using the norm notation we get

$$2\tilde{\omega}p_j(\|\mathbf{U}_1\|_{M_\Sigma}^2 + \|\mathbf{U}_2\|_{M_\Sigma}^2) + \tilde{\omega}\tilde{\sigma}\|\mathbf{U}_1 + \mathbf{U}_2\|_{M_\Sigma}^2 = 0.$$

From this last equation, we see that $\mathbf{U}_j = 0$, since all the terms are positive, which proves the equivalence between (4.27) and (4.24). ∎

Algorithm	$\mathcal{F}(\tilde{S}_j)$
1	0
2	$-\frac{s-i\tilde{\omega}}{s+i\tilde{\omega}}, \qquad s \in \mathbb{C}$
3	$-\frac{k^2+i\tilde{\omega}\tilde{\sigma}}{k^2-2\tilde{\omega}^2+i\tilde{\omega}\tilde{\sigma}+2i\tilde{\omega}s}, \qquad s \in \mathbb{C}$
4	$-\frac{s_j-i\tilde{\omega}}{s_j+i\tilde{\omega}}, \quad s_j \in \mathbb{C}$
5	$-\frac{k^2+i\tilde{\omega}\tilde{\sigma}}{k^2-2\tilde{\omega}^2+i\tilde{\omega}\tilde{\sigma}+2i\tilde{\omega}s_j}, \quad s_j \in \mathbb{C}$

Table 5.1: Symbols of the different operators

	without overlap	
Algorithm	ρ	parameters
1	$1-\frac{\tilde{\omega}^2\tilde{\sigma}}{C^3}h^3$	none
2	$1-\frac{2^{\frac{3}{4}}(\tilde{\omega}\tilde{\sigma})^{\frac{1}{4}}\sqrt{h}}{\sqrt{C}}$	$p=\frac{(\tilde{\omega}\tilde{\sigma})^{\frac{1}{4}}\sqrt{C}}{2^{\frac{1}{4}}\sqrt{h}}$
3	$1-\frac{2^{\frac{11}{7}}(\tilde{\omega}^4\tilde{\sigma}^2)^{\frac{1}{14}}h^{\frac{3}{7}}}{3^{\frac{3}{7}}C^{\frac{3}{7}}}$	$p=\frac{2^{\frac{4}{7}}(\tilde{\omega}^4\tilde{\sigma}^2)^{\frac{1}{14}}C^{\frac{4}{7}}}{3^{\frac{3}{7}}h^{\frac{4}{7}}}$
4	$1-\frac{(2\,\tilde{\omega}\,\tilde{\sigma})^{\frac{1}{8}}h^{\frac{1}{4}}}{C^{\frac{1}{4}}}$	$p_1=\frac{(2\,\tilde{\omega}\,\tilde{\sigma})^{\frac{1}{8}}C^{\frac{3}{4}}}{h^{\frac{3}{4}}}$, $p_2=\frac{(2\,\tilde{\omega}\,\tilde{\sigma})^{3/8}C^{1/4}}{2\,h^{\frac{1}{4}}}$
5	$1-\frac{2^{\frac{34}{13}}(\tilde{\omega}^4\tilde{\sigma}^2)^{\frac{1}{26}}h^{\frac{3}{13}}}{3^{\frac{3}{13}}C^{\frac{3}{13}}}$	$p_1=\frac{2^{\frac{8}{13}}(\tilde{\omega}^4\tilde{\sigma}^2)^{\frac{1}{26}}C^{\frac{10}{13}}}{3^{\frac{3}{13}}h^{\frac{10}{13}}}$, $p_2=\frac{2^{\frac{11}{13}}(\tilde{\omega}^4\tilde{\sigma}^2)^{\frac{3}{26}}C^{\frac{4}{13}}}{3^{\frac{9}{13}}h^{\frac{4}{13}}}$

Table 5.2: Asymptotic convergence factor and optimal choice of the parameters in the transmission conditions.

5. Numerical results. We illustrate the performance of the optimized Schwarz algorithms discretized using a DG method in two dimensions. We consider the TM formulation of Maxwell's equations, i.e. $\mathbf{E}=(0,0,E_z)^T$ and $\mathbf{H}=(H_x,H_y,0)^T$. We can then rewrite the algorithm (3.1) by using that now $\mathbf{W}=(E_z,H_x,H_y)^T$, and the corresponding G-matrices are

$$G_0=\begin{pmatrix}\tilde{\sigma}+i\tilde{\omega} & 0_{1\times 2}\\ 0_{2\times 1} & i\tilde{\omega}\mathbb{I}_{2\times 2}\end{pmatrix}, \quad G_x=\begin{pmatrix}0 & N_{\mathbf{e}_x}\\ N_{\mathbf{e}_x}^T & 0\end{pmatrix}, \quad G_y=\begin{pmatrix}0 & N_{\mathbf{e}_y}\\ N_{\mathbf{e}_y}^T & 0\end{pmatrix},$$

where $N_{\mathbf{n}}=(n_y,-n_x)^T$. We give in Table 5.1 the corresponding Fourier symbols of $\tilde{S}_j$ in the two-dimensional case, which were derived from the 3d results given in [18]. The parameters $s=p(1+i)$, $s_1=p_1(1+i)$ and $s_2=p_2(1+i)$ are solutions of specific min-max problems solved in [18], and their asymptotic behavior in the homogeneous non-overlapping case is shown in Table 5.2, together with the corresponding convergence factors and the constant C is defined such that $k_{\max}=\frac{C}{h}$ is the highest numerical frequency that can be represented by the discretization method on a mesh with mesh size h.

The Fourier symbols of the operators in Algorithms 1, 2 and 4 are constants, therefore their expression is the same in physical space. In this case (3.8) can be written in the 2d situation considered here as

$$\begin{cases} E_1^{n+1}-N_{\mathbf{n}}\mathbf{H}_1^{n+1}+\tilde{S}_1(E_1^{n+1}+N_{\mathbf{n}}\mathbf{H}_1^{n+1})=E_2^n-N_{\mathbf{n}}\mathbf{H}_2^n+\tilde{S}_1(E_2^n+N_{\mathbf{n}}\mathbf{H}_2^n),\\ E_2^{n+1}+N_{\mathbf{n}}\mathbf{H}_2^{n+1}+\tilde{S}_2(E_2^{n+1}-N_{\mathbf{n}}\mathbf{H}_2^{n+1})=E_1^n+N_{\mathbf{n}}\mathbf{H}_1^n+\tilde{S}_2(E_1^n-N_{\mathbf{n}}\mathbf{H}_1^n).\end{cases} \tag{5.1}$$

This is not the case for algorithms 3 and 5, where second order transmission conditions result, because k^2 appears in the corresponding Fourier symbols. As in the 3d case, we need to rewrite the transmission conditions: the $\tilde{S}_j$ are operators whose Fourier symbol can be written as

$$\mathcal{F}(\tilde{S}_j) = \frac{q_j(k)}{r_j(k)} \text{ with } q_j(k) = -(k^2 + i\tilde{\omega}\tilde{\sigma}),\ r_j(k) = k^2 - 2\tilde{\omega}^2 + i\tilde{\omega}\tilde{\sigma} + 2i\tilde{\omega}s_j.$$

We see that for the numerator and denominator separately, $\mathcal{F}^{-1}(q_j)$ and $\mathcal{F}^{-1}(r_j)$ are partial differential operators in the tangential direction,

$$\mathcal{F}^{-1}q_j = \partial_{\tau\tau} - i\tilde{\omega}\tilde{\sigma},\ \mathcal{F}^{-1}r_j = -\partial_{\tau\tau} - 2\tilde{\omega}^2 + i\tilde{\omega}\tilde{\sigma} + 2i\tilde{\omega}s_j.$$

In this case, we multiply the transmission conditions on both sides by the denominator, and the interface iteration (5.1) can then be re-written as

$$\left\{\begin{array}{rcl} \mathcal{F}^{-1}r_1(E_1^{n+1} - N_{\mathbf{n}}\mathbf{H}_1^{n+1}) & + & \mathcal{F}^{-1}q_1(E_1^{n+1} + N_{\mathbf{n}}\mathbf{H}_1^{n+1}) \\ & = & \mathcal{F}^{-1}r_1(E_2^{n} - N_{\mathbf{n}}\mathbf{H}_2^{n}) + \mathcal{F}^{-1}q_1(E_2^{n} + N_{\mathbf{n}}\mathbf{H}_2^{n}), \\ \mathcal{F}^{-1}r_2(E_2^{n+1} + N_{\mathbf{n}}\mathbf{H}_2^{n+1}) & + & \mathcal{F}^{-1}q_2(E_2^{n+1} - N_{\mathbf{n}}\mathbf{H}_2^{n+1}) \\ & = & \mathcal{F}^{-1}r_2(E_1^{n} + N_{\mathbf{n}}\mathbf{H}_1^{n}) + \mathcal{F}^{-1}q_2(E_1^{n} - N_{\mathbf{n}}\mathbf{H}_1^{n}), \end{array}\right. \tag{5.2}$$

similarly to the general 3d case we explained in (4.15).

5.1. Plane wave in a homogeneous conductive medium. We consider first the propagation of a plane wave in a homogeneous conductive medium. The computational domain is $\Omega = (0,1)^2$, and $\tilde{\sigma} = 0.5$. We use DG discretizations with several polynomial orders, denoted by DG-$\mathbb{P}_k$, with $k = 1, 2, 3, 4$, and impose on $\partial\Omega = \Gamma_a$ an incident wave

$$\mathbf{W}_{\text{inc}} = \begin{pmatrix} \frac{k_y}{\tilde{\omega}} \\ \frac{-k_x}{\tilde{\omega}} \\ 1 \end{pmatrix} e^{-i\mathbf{k}\cdot\mathbf{x}},\ \text{and } \mathbf{k} = \begin{pmatrix} k_x \\ k_y \end{pmatrix} = \begin{pmatrix} \tilde{\omega}\sqrt{1 - i\frac{\tilde{\sigma}}{\tilde{\omega}}} \\ 0 \end{pmatrix}. \tag{5.3}$$

The domain Ω is decomposed into two subdomains $\Omega_1 = (0, 0.5) \times (0, 1)$ and $\Omega_2 = (0.5, 1) \times (0, 1)$. The goal of this first test problem is to retrieve numerically the asymptotic behavior of the convergence factors of the optimized Schwarz methods when discretized using DG, and to compare with the theoretical convergence factors shown in Table 5.2. The iteration numbers to reduce the relative residual by six orders of magnitude are given in Table 5.3, where also the iteration numbers are given in parentheses for the use of the Schwarz methods as preconditioners for a Krylov method, which is BiCGStab in our case. We clearly see that there is a hierarchy of faster and faster algorithms, and their asymptotic behavior corresponds well to the analysis, as one can see from Figure 5.1.

5.2. Plane wave in a multi-layer heterogeneous medium. We study now the performance of the optimized Schwarz algorithms in the case of a heterogeneous propagation medium. The model problem we consider is the propagation of a plane wave in a multi-layer conductive medium, as shown in Figure 5.2 on the left. We decompose the computational domain $\Omega = (-1, 1)^2$ into two subdomains $\Omega_1 = (0, 0.5) \times (0, 1)$ and $\Omega_2 = (0.5, 1) \times (0, 1)$, as shown in Figure 5.2 on the right. The electromagnetic characteristics of the medium are given in Table 5.4.

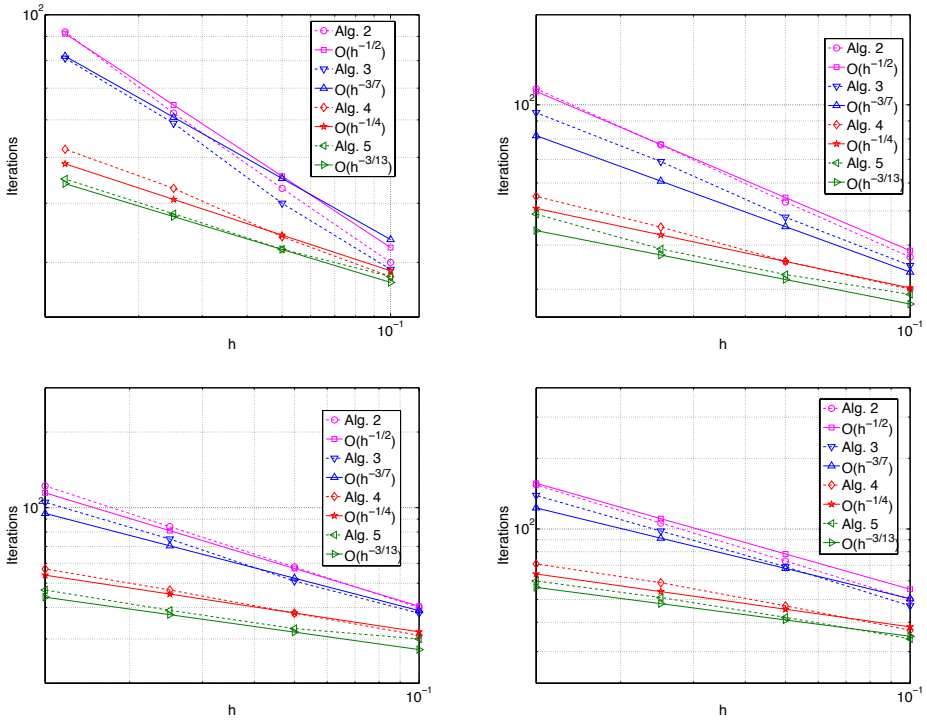

Fig. 5.1: Asymptotic behavior of the iteration numbers from Table 5.3 as a function of the mesh size h for the DG-$\mathbb{P}_1$, DG-$\mathbb{P}_2$, DG-$\mathbb{P}_3$,and DG-$\mathbb{P}_4$ discretizations.

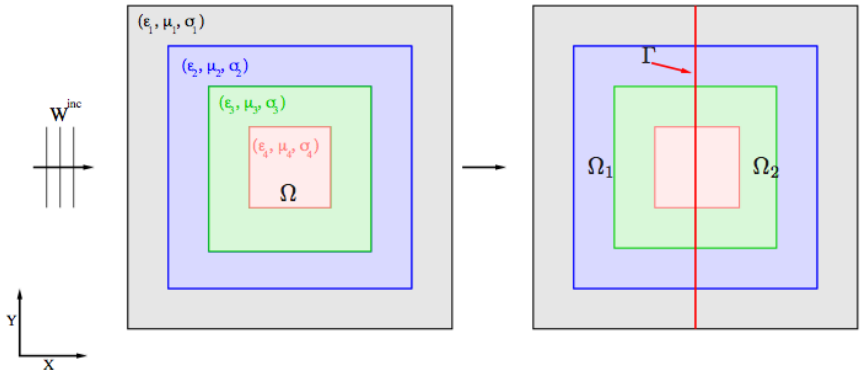

Fig. 5.2: Domain configuration for the model problem of scattering of a plane wave in a multi-layer domain.

h	$\frac{1}{10}$	$\frac{1}{20}$	$\frac{1}{40}$	$\frac{1}{80}$
DG-$\mathbb{P}_1$, $\tilde{\omega} = 2\pi$				
Algorithm 1	383 (16)	1396 (21)	5434 (27)	24400 (35)
Algorithm 2	30 (9)	43 (11)	62 (13)	92 (18)
Algorithm 3	29 (9)	40 (10)	59 (13)	81 (18)
Algorithm 4	28 (10)	34 (10)	43 (12)	52 (17)
Algorithm 5	28 (9)	32 (9)	38 (10)	45 (15)
DG-$\mathbb{P}_2$, $\tilde{\omega} = 10/3\pi$				
Algorithm 1	1573 (21)	2288 (24)	10520 (29)	55054 (35)
Algorithm 2	37 (11)	53 (12)	77 (16)	111 (18)
Algorithm 3	35 (10)	48(11)	69 (16)	95 (17)
Algorithm 4	30 (10)	36 (12)	45 (14)	55 (16)
Algorithm 5	29 (9)	33 (10)	39 (13)	49 (14)
DG-$\mathbb{P}_3$, $\tilde{\omega} = 13/3\pi$				
Algorithm 1	650 (21)	3025 (25)	17900 (30)	(51)
Algorithm 2	40 (11)	58 (14)	84 (16)	122 (21)
Algorithm 3	38 (11)	51 (13)	75 (15)	105 (19)
Algorithm 4	31 (10)	38 (13)	47 (15)	57 (19)
Algorithm 5	30 (9)	33 (11)	39 (13)	47 (16)
DG-$\mathbb{P}_4$, $\tilde{\omega} = 6\pi$				
Algorithm 1	1072 (29)	6318 (38)	39977 (51)	(64)
Algorithm 2	50 (12)	73 (15)	106 (18)	154 (21)
Algorithm 3	47 (11)	69 (14)	98 (18)	139 (20)
Algorithm 4	37 (12)	47 (14)	59 (17)	71 (19)
Algorithm 5	34 (10)	42 (12)	51 (15)	60 (17)

Table 5.3: Wave propagation in a homogeneous medium. Iteration count as a function of h when the optimized Schwarz methods are used as iterative solvers, and in parentheses when used as preconditioners.

Layer i	ε_i	$\tilde{\sigma}_i$	μ_i	DG-$\mathbb{P}_i$
1	1.0	0.0	1	1
2	2.25	0.1	1	2
3	3.5	0.2	1	3
4	5.3	0.5	1	4

Table 5.4: Characteristic parameters of the medium for the model problem of scattering of a plane wave in a multi-layer domain.

We test here the method DG-$\mathbb{P}_{1,2,3,4}$ where the interpolation degree is fixed for each element of the mesh according to the local wavelength, see the last column in Table 5.4. We show again the iteration numbers we obtain from the various optimized Schwarz algorithms to reduce the relative residual by 6 orders of magnitude in Table 5.5, and the corresponding iteration numbers when the Schwarz methods are used as

h	$\frac{1}{20}$	$\frac{1}{40}$	$\frac{1}{80}$	$\frac{1}{160}$
Algorithm 1	727 (31)	2974 (41)	11973 (52)	(70)
Algorithm 2	108 (21)	153(25)	220 (30)	315 (33)
Algorithm 3	101 (20)	138 (23)	197 (27)	267 (30)
Algorithm 4	87 (18)	103 (22)	128 (25)	157 (28)
Algorithm 5	84 (16)	96 (20)	113 (22)	140 (25)

Table 5.5: Scattering of a plane wave in a multi-layer domain. Iteration count as a function of h when the optimized Schwarz methods are used as iterative solvers, and in parentheses when used as preconditioners.

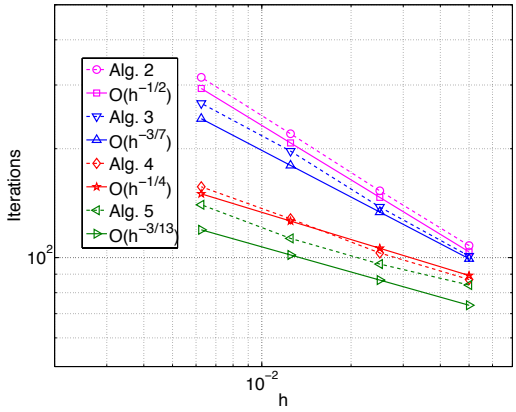

Fig. 5.3: Asymptotic behavior of the iteration numbers from Table 5.5 as a function of the mesh size h.

preconditioners in parentheses. In Figure 5.3, we plot these iteration numbers as a function of the mesh size, and also the corresponding theoretical asymptotic iteration number counts, which shows that even in such a layered medium, where our analysis is not valid any more, the Schwarz algorithms still behave asymptotically as the constant medium theory indicates. We finally show in 5.4 the real part of the electric field for this scattering problem.

5.3. Scattering of a plane wave by a conductive dielectric cylinder. The final model problem we consider is the scattering of a plane wave by a dielectric conductive cylinder with radius $r_0 = 0.6$ m. The computational domain is obtained by artificially restricting the domain to a cylinder with radius $r = 1.6$ m, and using the Silver-Müller condition on the artificial boundary. We use a non-uniform triangular mesh which consists of 2078 vertices and 3958 triangles, see Figure 5.5. The relative permittivity of the inner cylinder is set to $\varepsilon_r = 2.25$ and its electric conductivity to $\tilde{\sigma} = 0.01$, while vacuum is assumed for the rest of the domain. The frequency we consider is F=300 MHz. Numerical simulations are performed using decompositions into 4 and 16 subdomains, for an example see Figure 5.5. We show the iteration numbers for the various optimized Schwarz methods to reduce the relative residual by

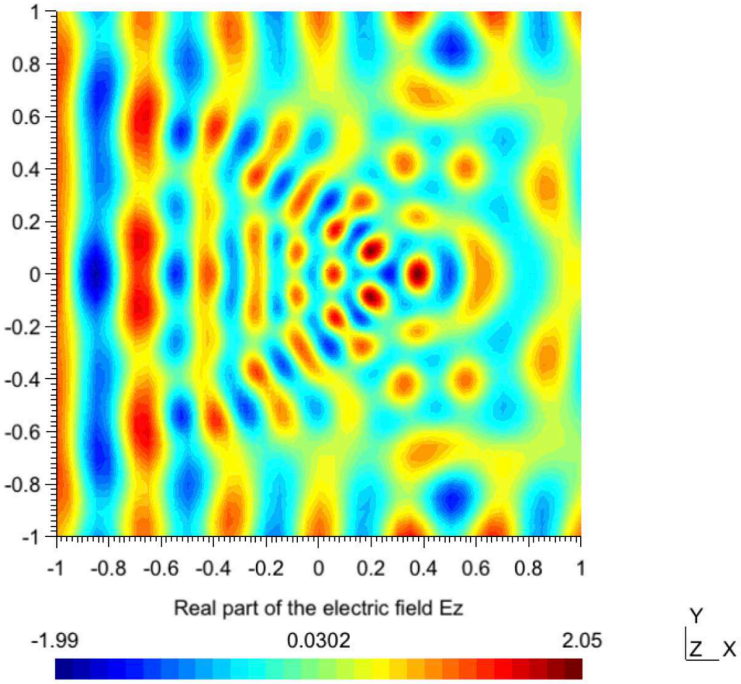

Fig. 5.4: Real part of the electric field for the scattering of a plane wave in a multi-layer domain.

6 orders of magnitude in Table 5.6. Here, DG-$\mathbb{P}_{1,2,3,4}$ stands for a non-uniform order DG discretization, i.e. the interpolation order is defined on an elementwise basis: small elements use low order shape functions, and large elements use high order ones. We note that the optimized algorithms improve substantially the convergence of the classical Schwarz algorithm (Algorithm 1 in the table) and also that the gain between both the optimized and the classical algorithms seems to slightly increase with the interpolation order. Finally, we also observe, as could be expected, a dependence of the iteration count on the number of subdomains, since we are not using any coarse grid correction in these experiments.

6. Conclusions. We have shown in this paper how optimized Schwarz methods can be properly discretized in the framework of DG-methods, such that at convergence, the result of the underlying DG mono-domain solution is recovered. The key idea is to introduce additional trace variables on each subdomain interface representing the DG-traces of the neighboring subdomain interface traces, and then to use both traces appropriately to discretize the optimized transmission conditions. We have tested the performance of the DG-discretized Schwarz methods on many numerical scattering experiments, both for homogeneous and heterogeneous media, and in various physical configurations and for various decompositions. Our numerical results indicate that the asymptotic performance of these algorithms obtained at a theoretical level for homogeneous media and constant coefficients well predicts the performance

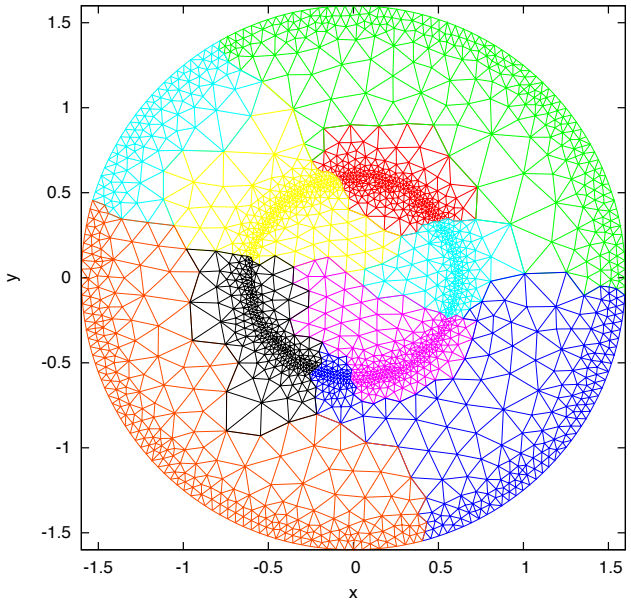

Fig. 5.5: Mesh and subdomain decomposition for the scattering problem of a plane wave by a dielectric conductive cylinder.

Method	Algo 1	Algo 2	Algo 3	Algo 4	Algo 5	# of domains
DG-$\mathbb{P}_1$	76	33	32	29	28	4
-	104	50	47	45	42	16
DG-$\mathbb{P}_2$	99	40	38	36	33	4
-	145	62	57	53	50	16
DG-$\mathbb{P}_3$	124	50	46	44	40	4
-	168	66	62	58	55	16
DG-$\mathbb{P}_4$	134	52	48	42	39	4
-	203	81	75	70	76	16
DG-$\mathbb{P}_{1,2,3,4}$	78	34	31	29	28	4
-	105	51	48	46	44	16

Table 5.6: Scattering of a plane wave by a dielectric conductive cylinder. Iteration count vs. mesh size.

of the algorithms when discretized using DG-discretizations, both in homogeneous and heterogeneous media, and for very general decompositions.

REFERENCES

[1] A. Alonso-Rodriguez and L. Gerardo-Giorda. New nonoverlapping domain decomposition methods for the harmonic Maxwell system. *SIAM J. Sci. Comput.*, 28(1):102–122, 2006.

[2] D. Arnold, F. Brezzi, B. Cockburn, and L. Marini. Unified analysis of Discontinuous Galerkin methods for elliptic problems. *SIAM J. Numer. Anal.*, 39(5):1749–1779, 2002.

[3] D. N. Arnold. An interior penalty finite element method with discontinuous elements. *SIAM Journal on Numerical Analysis*, 19(4):pp. 742–760, 1982.

[4] M. E. Bouajaji, V. Dolean, M. J. Gander, S. Lanteri, and R. Perrussel. DG discretization of optimized Schwarz methods for Maxwell's equations. In J. Erhel, M. J. Gander, L. Halpern, T. Sassi, and O. Widlund, editors, *Proceedings of the 21st international domain decomposition conference*. Springer LNCSE, 2013.

[5] A. Buffa, M. Costabel, and D. Sheen. On traces for H(curl, Ω) in Lipschitz domains. *Journal of Mathematical Analysis and Applications*, 276(2):845–867, 2002.

[6] A. Buffa and I. Perugia. Discontinuous Galerkin approximation of the Maxwell eigenproblem. *SIAM J. Numer. Anal.*, 44(5):2198–2226, 2006.

[7] P. Chevalier and F. Nataf. An OO2 (Optimized Order 2) method for the Helmholtz and Maxwell equations. In *10th International Conference on Domain Decomposition Methods in Science and in Engineering*, pages 400–407, Boulder, Colorado, USA, 1997. AMS.

[8] P. Collino, G. Delbue, P. Joly, and A. Piacentini. A new interface condition in the non-overlapping domain decomposition for the Maxwell equations. *Comput. Methods Appl. Mech. Engrg.*, 148:195–207, 1997.

[9] B. Després. Décomposition de domaine et problème de Helmholtz. *C.R. Acad. Sci. Paris*, 1(6):313–316, 1990.

[10] B. Després, P. Joly, and J. Roberts. A domain decomposition method for the harmonic Maxwell equations. In *Iterative methods in linear algebra*, pages 475–484, Amsterdam, 1992. North-Holland.

[11] B. Després, P. Joly, and J. E. Roberts. A domain decomposition method for the harmonic Maxwell equations. In *Iterative methods in linear algebra (Brussels, 1991)*, pages 475–484, Amsterdam, 1992. North-Holland.

[12] V. Dolean, H. Fol, S. Lanteri, and R. Perrussel. Solution of the time-harmonic Maxwell equations using discontinuous Galerkin methods. *J. Comput. Appl. Math.*, 218(2):435–445, 2008.

[13] V. Dolean, M. J. Gander, S. Lanteri, J.-F. Lee, and Z. Peng. Optimized Schwarz methods for curl-curl time-harmonic Maxwell's equations. In J. Erhel, M. J. Gander, L. Halpern, T. Sassi, and O. Widlund, editors, *Proceedings of the 21st international domain decomposition conference*. Springer LNCSE, 2013.

[14] V. Dolean, M. J. Gander, J.-F. Lee, and Z. Peng. Effective Transmission Conditions for Domain Decomposition Methods applied to the Time-Harmonic Curl-Curl Maxwell's equations. *submitted*, 2014.

[15] V. Dolean, L. Gerardo-Giorda, and M. J. Gander. Optimized Schwarz methods for Maxwell equations. *SIAM J. Scient. Comp.*, 31(3):2193–2213, 2009.

[16] V. Dolean, S. Lanteri, and R. Perrussel. A domain decomposition method for solving the three-dimensional time-harmonic Maxwell equations discretized by discontinuous Galerkin methods. *J. Comput. Phys.*, 227(3):2044–2072, 2008.

[17] V. Dolean, S. Lanteri, and R. Perrussel. Optimized Schwarz algorithms for solving time-harmonic Maxwell's equations discretized by a discontinuous Galerkin method. *IEEE. Trans. Magn.*, 44(6):954–957, 2008.

[18] M. El Bouajaji, V. Dolean, M. J. Gander, and S. Lanteri. Optimized Schwarz methods for the time-harmonic Maxwell equations with dampimg. *SIAM J. Scient. Comp.*, 34(4):2048–2071, 2012.

[19] O. Ernst and M. Gander. Why it is difficult to solve Helmholtz problems with classical iterative methods. In I. Graham, T. Hou, O. Lakkis, and R. Scheichl, editors, *Numerical Analysis of Multiscale Problems*, pages 325–363. Springer Verlag, 2012.

[20] M. J. Gander, F. Magoulès, and F. Nataf. Optimized Schwarz methods without overlap for the Helmholtz equation. *SIAM J. Sci. Comput.*, 24(1):38–60, 2002.

[21] P. Helluy. *Résolution numérique des équations de Maxwell harmoniques par une méthode d'éléments finis discontinus*. PhD thesis, Ecole Nationale Supérieure de l'Aéronautique, 1994.

[22] P. Helluy and S. Dayma. Convergence d'une approximation discontinue des systèmes du premier ordre. *C. R. Acad. Sci. Paris*, 319:1331–1335, 1994.

[23] P. Helluy, P. Mazet, and P. Klotz. Sur une approximation en domaine non borné des équations de Maxwell instationnaires: comportement asymptotique. *La Recherche Aérospatiale*, 5:365–377, 1994.

[24] J. Hesthaven and T. Warburton. *Nodal Discontinuous Galerkin methods: algorithms, analysis and applications*. Springer, 2008.

[25] P. Houston, I. Perugia, A. Schneebeli, and D. Schötzau. Interior penalty method for the indefinite time-harmonic Maxwell equations. *Numer. Math.*, 100(3):485–518, 2005.

[26] P. Houston, I. Perugia, A. Schneebeli, and D. Schötzau. Mixed discontinuous Galerkin approximation of the Maxwell operator: the indefinite case. *ESAIM: Math. Model. Numer. Anal.*, 39(4):727–753, 2005.

[27] S.-C. Lee, M. Vouvakis, and J.-F. Lee. A non-overlapping domain decomposition method with non-matching grids for modeling large finite antenna arrays. *J. Comput. Phys.*, 203(1):1–21, 2005.

[28] Z. Peng and J.-F. Lee. Non-conformal domain decomposition method with second-order transmission conditions for time-harmonic electromagnetics. *J. Comput. Phys.*, 229(16):5615–5629, 2010.

[29] Z. Peng and J.-F. Lee. A scalable nonoverlapping and nonconformal domain decomposition method for solving time-harmonic maxwell equations in r^3. *SIAM Journal on Scientific Computing*, 34(3):A1266–A1295, 2012.

[30] Z. Peng, V. Rawat, and J.-F. Lee. One way domain decomposition method with second order transmission conditions for solving electromagnetic wave problems. *J. Comput. Phys.*, 229(4):1181–1197, 2010.

[31] I. Perugia, D. Schötzau, and P. Monk. Stabilized interior penalty methods for the time-harmonic Maxwell equations. *Comput. Methods Appl. Mech. Engrg.*, 191(41-42):4675–4697, 2002.

[32] V. Rawat. *Finite Element Domain Decomposition with Second Order Transmission Conditions for Time-Harmonic Electromagnetic Problems*. PhD thesis, Ohio State University, 2009.

[33] V. Rawat and J.-F. Lee. Nonoverlapping domain decomposition with second order transmission condition for the time-harmonic Maxwell's equations. *SIAM J. Sci. Comput.*, 32(6):3584–3603, 2010.